X-RAY MEASUREMENT OF RESIDUAL STRESSES

by

MYUNG CHUL KIM

B. S., Seoul National University, 1964

A MASTER'S THESIS

submitted in partial fulfillment of the

requirements for the degree

MASTER OF SCIENCE

Department of Industrial Engineering

KANSAS STATE UNIVERSITY
Manhattan, Kansas

1968

Approved by:

A E Hostetter

Major Professor

TABLE OF CONTENTS

	Page
INTRODUCTION	1
THEORY	4
EXPERIMENTAL PROCEDURE	8
I. Material	8
II. Test Apparatus and Special Fixture	8
III. Technique	10
RESULTS AND DISCUSSION	19
APPENDIX I	31
APPENDIX II	38
APPENDIX III	41
APPENDIX IV	44
APPENDIX V	46
REFERENCES	47
ACKNOWLEDGMENTS	
ABSTRACT	

INTRODUCTION

Residual stresses frequently called "locked-up" stresses or "internal" stresses, have been defined by Orowan (1) as those existing in bodies upon which no external forces are acting. Residual stresses are developed in metals to some degree by every commercial fabricating process: welding, casting, heat treating, forming, machining, grinding, plating, and others. Specifically they can arise out of unequal plastic deformation, causing misfit of solute atoms and dislocations on removal of the load; or a chemical change, for instance, may alter a part of the body and similarly produce residual stresses. There are also many other ways of creating these stresses.

Residual stresses generally fall into two categories. First, those which result when external factors influence differently various parts of a body. Thus, even though the material may be isotropic and homogeneous, residual stresses may be produced. Secondly, textural inhomogeneities of the material may give rise to internal stresses from external influences which are acting uniformly upon the body. The residual stresses of the first group, arising for example out of a deformation or cutting process, are often large and well defined in their distribution. They are called macrostresses. The other group contains residual stresses (caused, for example, by quenching a two-phase alloy) which are usually on a granular scale and often randomly distributed. These are termed microstresses, or residual stresses of the second kind. The microstresses are, in general, uniformly tensile or compressive in a particular grain, but tentative suggestions of a subgranular variation have been made and have led to the idea of micro-

stresses of the third kind (2).

Residual stresses in metals have a technological importance because of their manifold and diverse effects. It is well understood that residual stresses play fundamental roles in plastic deformation, in crack initiation, in brittle fracture, and in fatigue crack growth (3). Depending on their nature and distribution in a metal, residual stresses can delay or hasten fatigue failures. Fortunately, the magnitude and direction of the residual stresses in metals, to some extent, can be changed so as to avoid difficulties or gain advantages. The removal or reduction in the intensity of residual stress is known as stress-relief. This may be accomplished either by heating or by mechanical working operations.

One of the main problems at present associated with the use of metals is that of residual stress. The passing of time has led to more powerful engines, more speed and a higher loading of parts and more concern with reliability. As indicated previously, residual stresses may be introduced either intentionally or accidentally as a result of mechanical, thermal, and metallurgical operations. This in turn has led to increased interest in residual stresses and their effects, both good and bad, on reliability and ultimate performance. Numerous investigations of measuring residual stresses have been made for the past decades (2). In recent years, the X-ray diffraction method has been the subject of considerable developmental work, and it has also been applied to a number of practical problems. Other stress measurement techniques in general are destructive to the part under study and thereby prohibit any normal service test on that part after the stress-

es have been evaluated. Another serious limitation to their use is the likelihood of introducing spurious stress during the necessary stock removal if the hardness of the sample is above very moderate levels. Many applications of the X-ray diffraction method of measuring residual stresses are being studied and numerous publications are available concerning these developments (2,4). The technique has proved quite successful in hardened high carbon steels from a practical point of view. However, there are still difficulties in reproducing the measurements from laboratory to laboratory and also from instrument to instrument.

Most stress measurement by X-ray diffraction has been performed using a two-exposure film method or a direct reading diffractometer. The purpose of this work is to develop the technique of counter diffractometer stress measurement by using a laboratory specimen. The work includes: (a) X-ray residual stress measurement of mild steel sheet, (b) the correlation of the data with mechanically determined values (strain gage data), (c) an examination and discussion of reproducibility, and (d) discussion of its applications.

THEORY

The X-ray diffraction method enables one to measure the distance between planes of atoms in metal crystals and thus to use the interplanar distance as a gage length for the determination of elastic strains at the surface. Therefore, the X-ray method is, as in other techniques, a measurement of strain and not stress. The method depends on the regularity of atomic planes. The interplanar spacing becomes a gage length which is altered proportionately by elastic stresses. Changes in interplanar spacing, produced by the stresses, divided by the original spacing (gage length) becomes an elastic strain. The strains measured are then converted to the stress by equations which can be developed from the classical theory of elasticity.

The theoretical or mathematical developments upon which the determination of stresses by X-ray diffraction techniques is based are presented in most textbooks on X-ray diffraction and are recapitulated in Appendix I. Figure 1 illustrates the basic two-exposure method of measuring residual stresses (or applied stresses). The interplanar spacing of a selected family of atomic planes in the phase under study is used as the indicator of elastic strain present. Since the penetration of the X-ray is practically limited to the surface of the order of a few thousandths of an inch, it may be assumed that the stresses for the region being investigated are parallel to the surface. The "d" is determined at two Ψ angular orientations of those planes to the surface direction in which it is desired to measure the stress. The common procedure is to determine the "d" value of the planes parallel to the surface---ψ equals 0^{o}---and again at some chosen angle of Ψ, usually

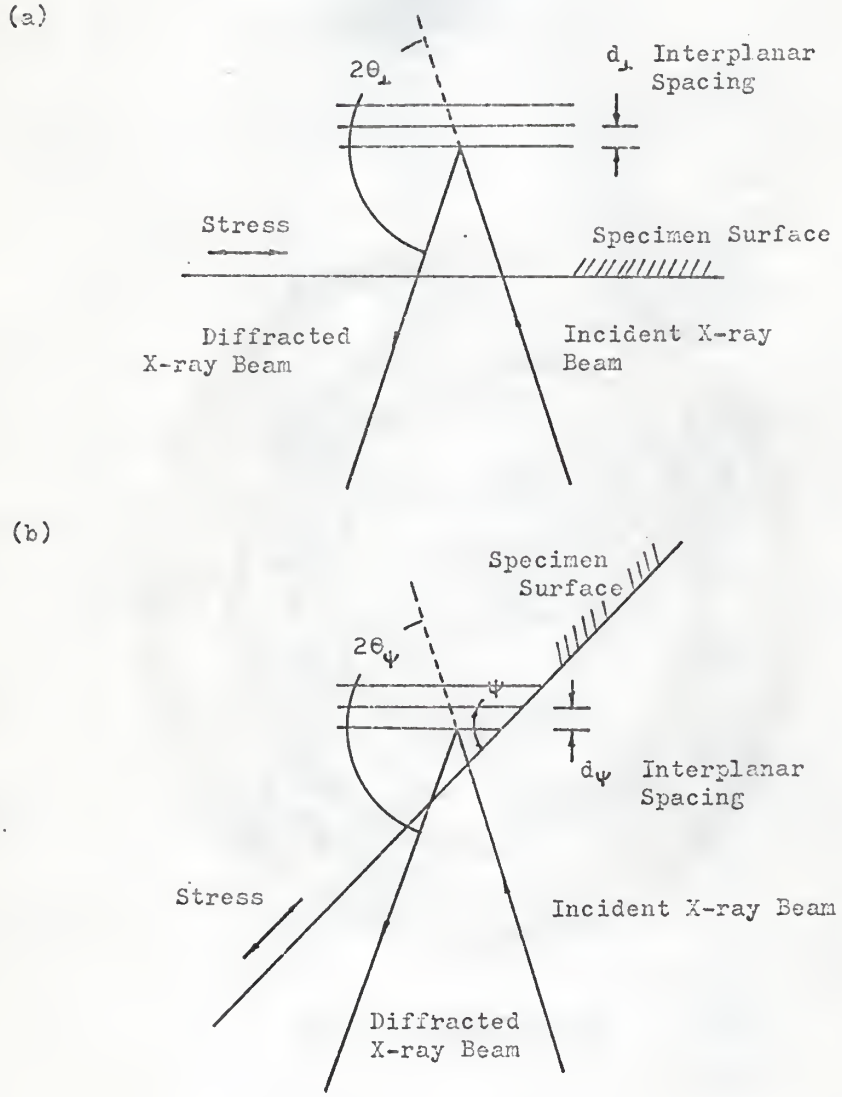

Fig. 1. Schematic arrangement for two-exposure method for determining residual stresses. (a) Measuring interplanar spacing for crystallographic planes parallel to surface. (b) Measuring spacing for planes at angle ψ to the surface.

45° or 60° to this direction (4).

The usual formula for the calculation of a residual stress (or an applied stress), σ, in a particular direction, φ, with respect to some arbitrary direction in a surface is (5)

$$\sigma_\varphi = \frac{E}{1+\nu} \cdot \frac{1}{\sin^2\psi} \cdot \frac{d_\psi - d_\perp}{d_\perp} \qquad 1.$$

where E is Young's modulus, ν is Poisson's ratio, ψ is the angle between the normal to the surface and the normal to the crystal planes whose spacing is d_ψ, obtained by inclining the incident X-ray beam to the surface, and $d_\perp$ is the spacing of crystal planes diffracting when the X-ray beam is incident normal to the surface. (Strictly speaking, $d_\perp$ should be the spacing between planes parallel to the surface of the specimen.) There are some assumptions made in the derivation of this formula; most basic, perhaps, is that the diffracting material is obeying the usual laws of elasticity for an isotropic, homogeneous medium. At the very surface, of course, the normal component is zero, and it is usually assumed that the depth of effective penetration of the X-rays is so slight that the normal component may be assumed to be zero. On the other hand, the stress components lying in the plane of the surface are assumed to be totally unaffected by the presence of the surface in so far as the X-ray diffraction measurements are concerned (6). Therefore, the X-ray technique is strictly valid for measurement of stress in a material which is elastic, homogeneous, and isotropic. It has been found that polycrystalline metals to a good approximation satisfy these requirements (4).

Either film or diffractometer X-ray diffraction techniques can be used for the measurement of the interplanar spacings. Changes in

spacings between planes parallel to the specimen surface and planes inclined at an angle ψ to the surface of the specimen can also be interpreted by changes in angular positions of the corresponding diffracted beams. When the measurements are made with a diffractometer, the data obtained are in terms of the angle of diffraction 2θ and it is convenient to express Eq. 1 in terms of 2θ. Thus:

$$\sigma_\varphi = \frac{E}{1+\nu} \cdot \frac{1}{\sin^2 \psi} \cdot \cot \theta \cdot \frac{(2\theta_\perp - 2\theta_\psi)}{2} \qquad 2.$$

where $2\theta_\perp$ is the observed value of the diffraction angle in the normal or $\psi = 0^\circ$ measurement and $2\theta_\psi$ is its value in the oblique or $\psi = \psi^\circ$ measurement. Since the cot θ may be assumed constant for small changes in the diffraction angle 2θ, Eq. 2 may be written as follows:

$$\sigma_\varphi = k(d_\psi - d_\perp) \text{ or } K(2\theta_\perp - 2\theta_\psi) \qquad 3.$$

This indicates that the stress is proportional to the shift in the diffraction angle 2θ as the angle ψ is changed.

The expression given above relating the residual stress, σ_φ, to the change in Bragg angle, θ, makes the assumption that E and ν are known constants, whereas in fact they vary considerably with crystallographic direction. Therefore, the use of these bulk (average) values in the computation of stress by X-ray measurements is open to criticism. Despite somewhat contradictory experimental findings (7,8), most investigators who have used X-rays consider that the average values of E and ν found from tensile tests induce no serious errors (4). For greatest accuracy, however, it was recommended that the constants should be determined for each material and experimental arrangement by making X-ray measurements on stress-relieved specimens subjected to known loads.

EXPERIMENTAL PROCEDURE

I. Material

A mild steel sheet (size: 2"x 1-3/8"x 1/16", approximately ASE 1010) used in this experiment was obtained from the Work Shop of the Department of Industrial Engineering, Kansas State University. A sample of the "as received" sheet probably in the hot-worked condition was given a 45 minutes annealing treatment at 1400°F and then furnace cooled without protective atmosphere. Scales formed at the specimen surface were removed by Descaler (4 oz/gal, 24 hours), and final surface preparation was performed by etching with dilute HCl (1:10) solution.

For instrumental checking, it was desirable that a "stress-free" sample be used. For this purpose, fine metallic filings was removed from the original sample and carefully annealed at 1300°F under the controlled atmosphere of argon and hydrogen gases. Since the particle size was very small, it possessed no macrostress, and, thus, was assumed to be stress-free.

II. Test Apparatus and Special Fixture

A Siemens Crystalloflex 4 counter diffractometer, two strain gages, and a Daytronic Strain Gage Plug-in Unit (Type 80) were used in this experiment. Because of the size and shape of the specimen, it was necessary to provide a special fixture to hold the specimen during the test. The physical layout of the goniometer may be visualized from the photograph in Fig. 2. The increments of strain were measured by two strain gages mounted on the front of the sample, while the X-ray measurements were taken at the portion between two strain gages.

All measurements herein reported were taken under the following

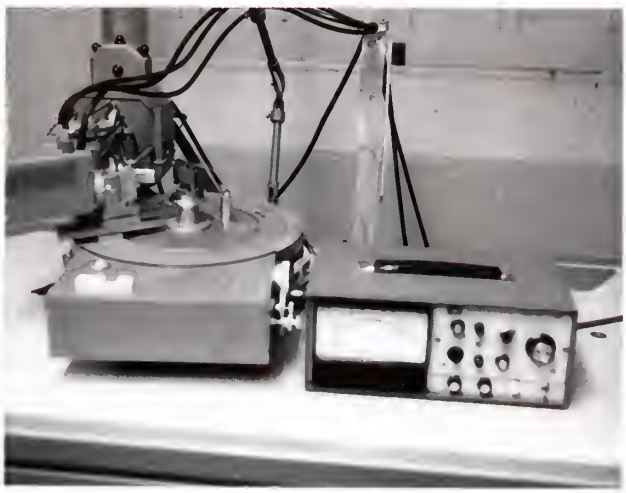

Fig. 2 X-ray Spectrogoniometer arrangement.

experimental conditions:

Counter Diffractometer

Tube	Chromium	Filter	Vanadium
Kv	35	Beam slit	2 mm
Ma	14	Detector slit	0.6 mm
Counter	Scintillation	Soller slit	Yes
Counter voltage	690		
Input sensitivity	80 per cent transmission		

Two Strain Gages

Gage factor	2.06 ± 1/2 per cent
Resistance	120 ± .2 ohm

III. Techique

The X-ray technique used in this experiment was adopted from those proposed by Christenson et al. (4) and may be summarized as follows:

A. Choice of Radiation and Filter

For residual stress measurements the radiation and reflecting planes are chosen such that the combination results in diffraction at the greatest possible value of θ commensurate with Bragg's Law and the physical limitations of the X-ray equipment employed. This provides for the greatest possible resolution of the diffracted beam. The optimum choice for the problem at hand is chromium (CrKα) radiation. The justifications are as follows:

The degree of diffraction line contrast is largely related to the success in achieving a monochromatic radiation. When a film tech-

nique is used, this is usually accomplished by placing a selective absorbing filter between the X-ray tube and specimen. The rule for choosing a suitable filter is this:

> "Pick for the filter an element whose K absorption edge is to the short-wavelength side of the Kα line of the target material."(9)

This filter is relatively effective in absorbing the Kβ radiation, as well as white radiation of this general wave-length. However, if a principal source of the background is fluorescent radiation from the sample, it is necessary to place the filter between the sample and film (or X-ray counter when the diffractometer is used). Choice of a proper material, relatively opaque to the fluoresced radiation is made with the aid of a table of X-ray absorption coefficients (4). This filter material must selectively absorb the fluorescent radiation from the sample and the Kβ radiation of the tube target material but not the Kα radiation of the tube target material.

The advantage of using chromium radiation with vanadium filter in the diffracted beam, especially for hardened steel, has been well demonstrated by Christenson and Rowland (10).

B. Parafocus Conditions

The usual diffractometer arrangement is shown in Fig. 3. In normal $\Psi = 0^{\circ}$ position, the sample surface is always at equal angles with the incident and diffracted beams so that radiation divergent from the source D is diffracted at all 2θ angles to a focus at A on the diffractometer circle. However, as shown in Fig. 3b, the focusing conditions are destroyed when the sample is rotated Ψ degrees such as $\Psi = 45^{\circ}$. This presents much difficulty if the ideal arrangement of continuously variable and accurately radial positioning of the counter slit are

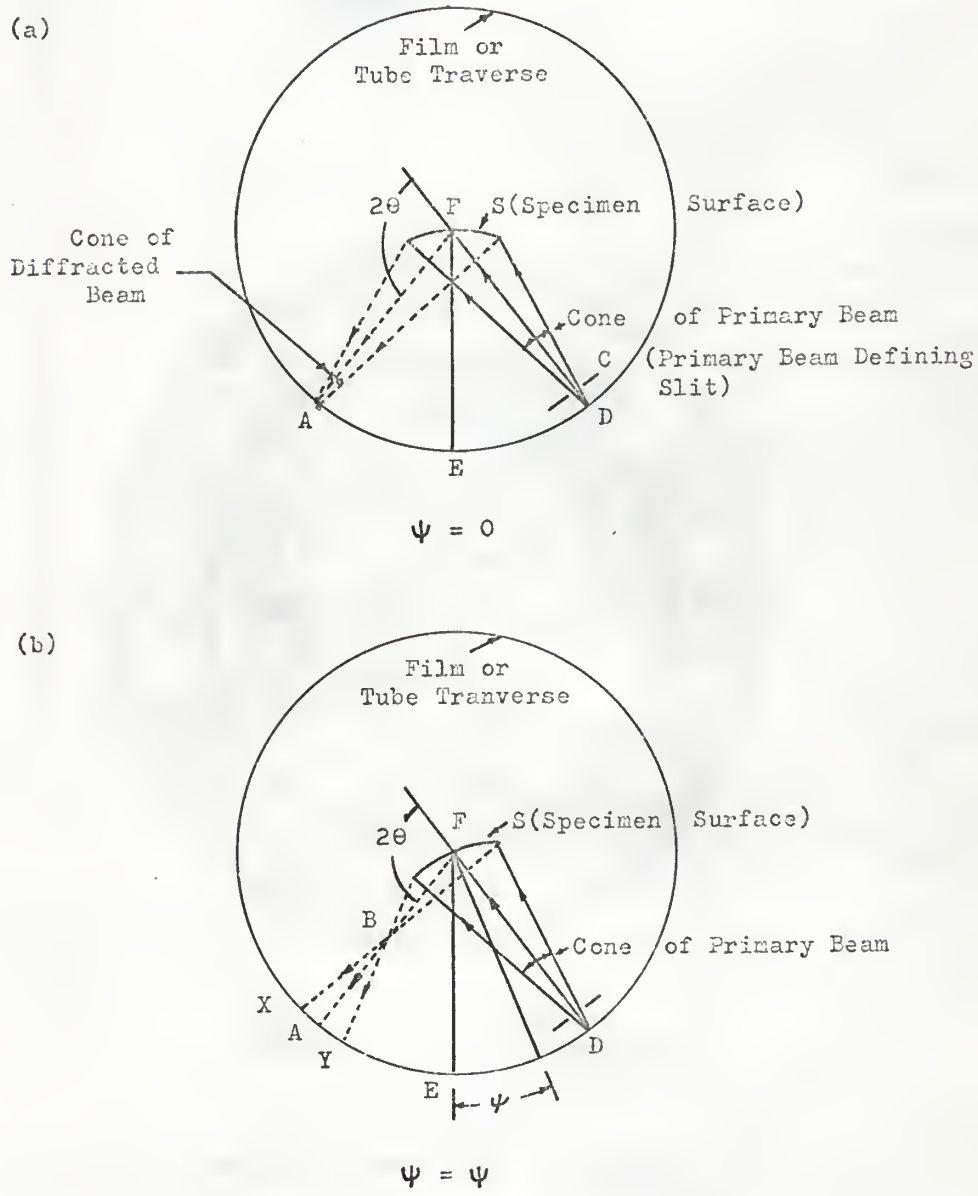

Fig. 3. Diffractometer focussing conditions: (a) with sample in normal $\psi = 0^{\circ}$, (b) with sample rotated ψ° from normal position.

attempted. Nevertheless, good parafocusing can be obtained if the counter slit is moved to a position on the focusing circle as described by Cullity (11).

The distance AB (see Fig. 3) which the counter slit must be moved toward the goniometer center is given by the following equation:

$$AB = R - R\frac{\cos(\Psi + \varphi)}{\cos(\Psi - \varphi)} \qquad 4.$$

where R is radius of goniometer circle (or source to sample distance), and $\varphi = 90^{\circ} - \theta$. Radiation parafocus settings in millimeters (mm) for Ψ angles of 45° and 60° at various 2θ angles in increments of 2θ are given in Appendix V.

C. Corrections of Line Measurements

The factors which affect X-ray diffraction line intensity are well established and discussed in most texts concerned with X-ray diffraction (5,9,11). The θ-dependent factors are known as the Polarization, Lorentz, and absorption factors. Since the incident X-ray beam is unpolarized, the Polarization intensity factor which arises in the Thomson equation for scattering by an electron may be written as follows:

$$P = \frac{(1 + \cos^2 2\theta)}{2}$$

This results in the scattered radiation being stronger in the forward and backward directions than in a direction at right angle to the primary beam.

The Lorentz factor comes from certain geometrical considerations. The total integrated intensity of a reflection from a given family of planes is characteristic of the sample material. However, the counter tube (or film) aperture, at any one 2θ position, receives only a

portion of this total integrated intensity which depends on the experimental arrangement. For the powder method, it has been shown that the Lorentz factor is:

$$L = \frac{1}{4 \sin^2 \theta \cos \theta}$$

In most tables of corrections for X-ray intensities, the Lorentz and Polarization factors are combined thus:

$$LP = \frac{1}{8} \cdot \frac{1 + \cos^2 2\theta}{\sin^2 \theta \cos \theta} \qquad 5.$$

and known as the Lorentz-Polarization factor. Values of this factor over the 2θ range used in this experiment are plotted on Fig. 4 and tabulated in Appendix IV.

The absorption factor is also a geometrical factor and is of importance when the mean path length of the X-rays within the sample varies with the angle of diffraction. The usual diffractometer arrangement in which the sample surface (or the tangent to the sample surface is at equal angles with the incident and diffracted beams ($\psi = 0^\circ$), makes the path length and hence the absorption factor constant and independent of the angle θ. However, at all specimen angles of ψ other than zero, the absorption becomes a function of the diffraction angle θ. Variation in the diffracted intensity with respect to angle θ may be written as follows:

$$I_d = k(1 - \tan \psi \cot \theta) \qquad 6.$$

Thus the θ dependent absorption factor is: $1 - \tan \psi \cot \theta$. In the case where ψ is set equal to 45°, for instance, the absorption factor is: $1 - \cot \theta$. The derivation of this relation is shown in Appendix III. It is further noted that this relationship does not apply to the

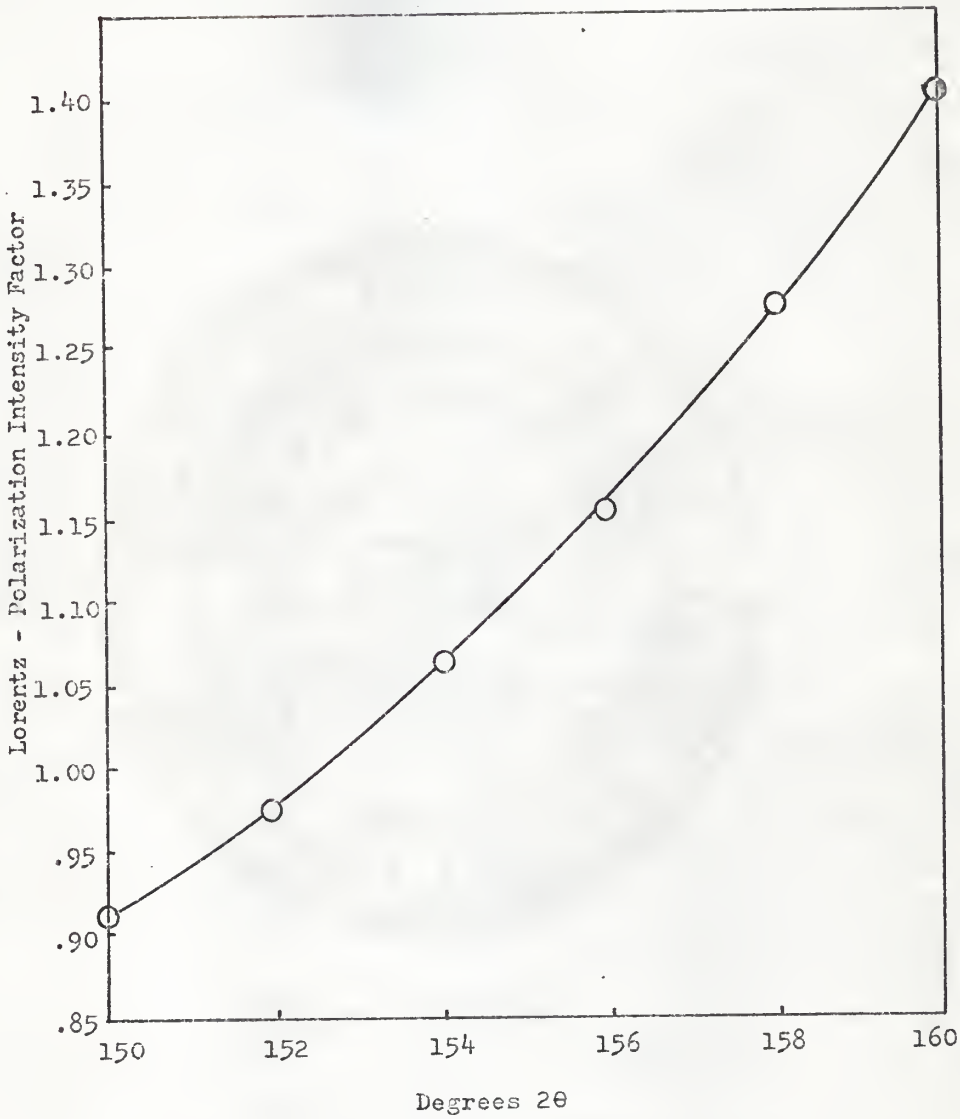

Fig. 4. Variation of relative intensity with angle 2θ resulting from Lorentz-Polarization factor.

common film techniques.

To simplify the correction procedure for angles of ψ other than zero, the LP and absorption factors were combined into a single correction factor and tabulated over the range of 2θ from 154° to 158° for ψ angles of 45° in Appendix IV.

D. Determination of Peak Position (Parabolic Method)

Once the necessary diffraction lines are obtained, the problem of how to measure them remains. The usefulness of the parabolic method is based on how well the diffraction peak is represented by a simple parabola. This in turn depends on the line symmetry. In order to determine the true peak position, several techniques such as centerline, line slope and parabolic methods have been developed by many investigators (8). However, the technique of fitting a parabola to three points on the diffraction peak, developed by Koistinen and Marburger (12), provided the most rigorous approach and is now believed to represent the best compromise between speed and accuracy of measurement.

Modern diffractometers are provided with both rate meter and scaler circuits. The rate meter, the output of which is automatically recorded as a function of the diffraction angle, provides a more or less instantaneous average of the X-ray diffraction intensity. The scaler circuit permits the accumulation and measure of the total number of X-ray counts or photons for a given interval of time or the measure of time required to accumulate a given number of counts. The former is called fixed-time scaling and provides a direct measure of X-ray intensities. The later is fixed-count scaling and results in the measure of inverse intensities. It has been found that fixed-count scaling is the better technique because it enables the choice and use of a constant

probable error (4).

In the three-point parabolic method, the peaks of the diffraction lines are fixed-count scaled at constant 2θ intervals suitable for outlining the particular lines being measured. Three initial measurements are made rapidly by accumulating only a relatively low number of counts (10,000 or less) at each 2θ position. From these data points, three positions of 2θ are selected for a more accurate determination of the inverse intensities. A final determination of the inverse intensities at each of the three points is obtained by accumulating 100,000 or more counts for each points. The measured inverse intensities are corrected for factors sensitive to 2θ by multiplying the inverse intensities by the appropriate factors listed in Appendix IV.

As indicated previously, LP factors are used to correct the data obtained at $\psi = 0^{\circ}$ and the combined LP-absorption factors are used at angles of ψ other than zero. Koistinen and Marburger (12) have also demonstrated that these correction procedures improve the line symmetry. After the points have been corrected, the vertex of the prabola that will fit these three points is computed by the following relation taken from Appendix II.

$$2\theta_{vertex} = 2\theta_1 + c\frac{(3a + b)}{(2a + 2b)} \qquad 7.$$

where $a = t_1 - t_2$

$b = t_3 - t_2$

t_1, t_2, t_3 = Time required to accumulate given number of counts at $2\theta_1$, $2\theta_2$, and $2\theta_3$

$c = 2\theta_2 - 2\theta_1$ or $2\theta_3 - 2\theta_2$

The computed vertex of the parabola is taken to be the best 2θ value

for the reflecting planes. Caution must be excercised, however, in using this parabolic method. For instance, the X-ray inverse intensity measurement at three points straddling the peak should be made at least 80 per cent up from background. This choice of points minimizes the effect of poor resoltution of the $K\alpha_1 - \alpha_2$ doublet (6). Furthermore, Koistinen and Marburger (12) also indicated that the peak positions are not seriously affected by the choice of angular position for the three data points, so long as the differences a and b are of the same sign.

RESULTS AND DISCUSSION

Typical data and computations are shown in Figs. 5 and 6, and Table 1. In Figs. 5 and 6, inverse intensities for both measurement at $\psi = 0^\circ$ and $\psi = 45^\circ$ were taken as the time (in seconds) required to count to 100,000 photons and are plotted against angular position in degrees 2θ over the most intense region of the $K\alpha_1$ peak. Since sharp diffraction lines with good resolution were available, three intensity points at equal 0.1° intervals were chosen and the intensity data had been corrected for the LP and absorption factor.

A principal objective of this work is to show that the X-ray method is capable of measuring increments of stress over the stress range below the elastic limit in bending. In order to demonstrate experimentally that the X-ray measurements of applied stress are linearly proportional to measurements made using strain gages, a special fixture which must be capable of changing the angle of incidence of the X-ray beam upon its surface independently of the position of the counter was made and is shown in Fig. 2. The specimen was fitted with two strain gages, above and below the radiated section of the specimen, to determine the average strain on the surface of the sample. A comparison of strain gage readings to X-ray data is given in Fig. 7, where the 45° line corresponds to perfect agreement. It was found that the combined errors of both methods produced a maximum deviation of just over 2000 psi when a published value of stress factor was used.

It has been emphasized that the X-ray stress measurement is the only reliable method for hardened or cold-worked metals and its reproducibility is within 3000 or 4000 psi (4). In the case of hardened

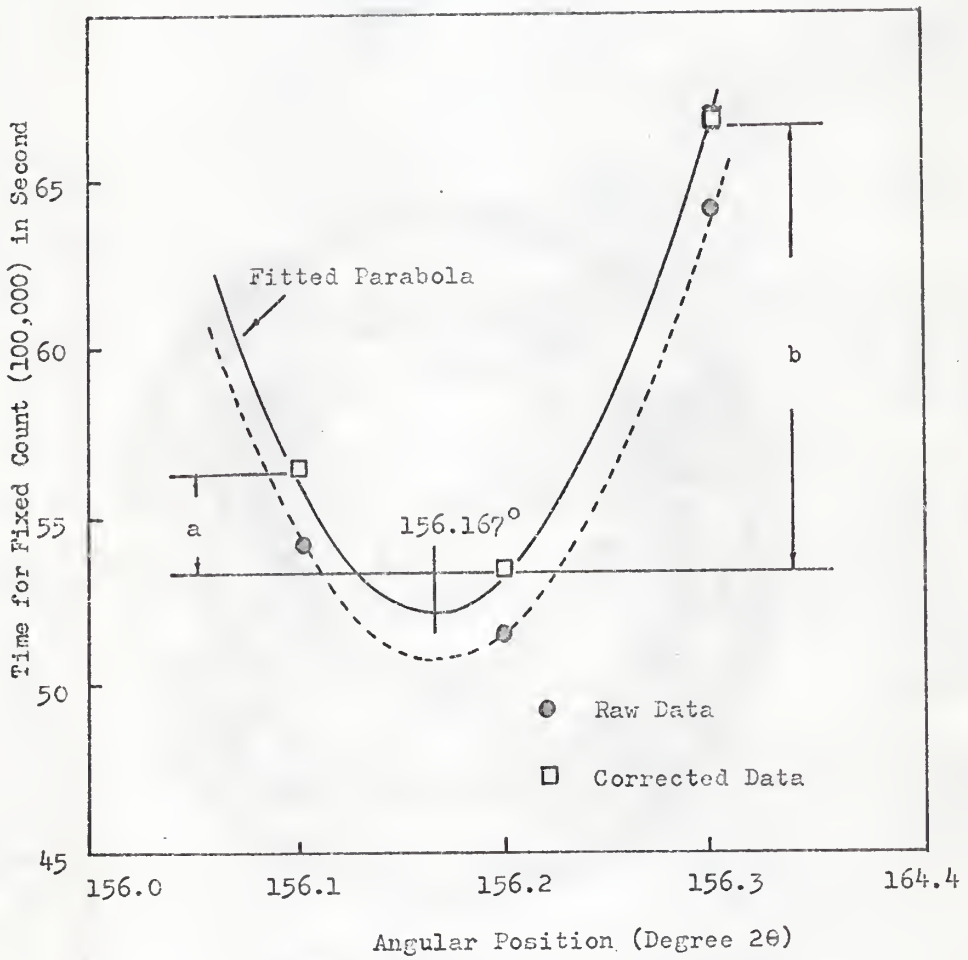

Fig. 5. Peak position as determined from a parabola fitted to corrected X-ray intensity data for $\psi = 0^{\circ}$.

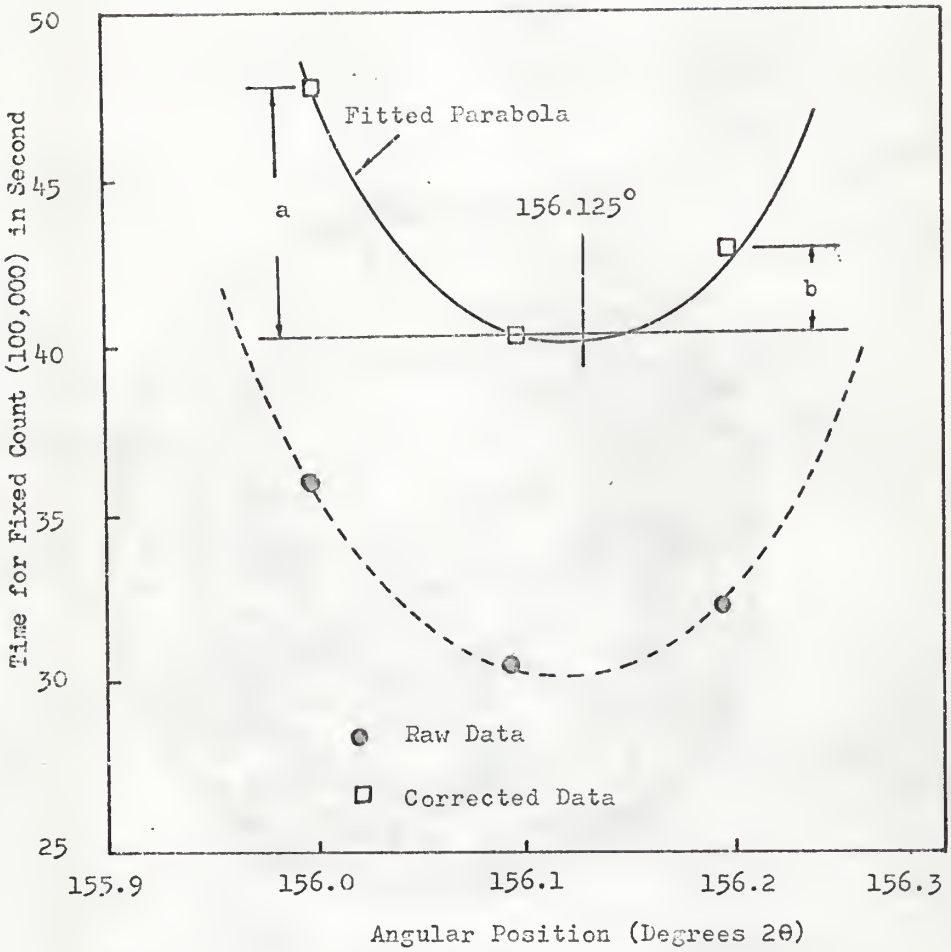

Fig. 6. Peak position as determined from a parabola fitted to corrected X-ray intensity data for $\psi = 45^{\circ}$.

Table 1

X-ray Measurement Of Residual Stresses
Data And Calculation Sheet

Mild Steel Sheet (Size: 2"x 1-3/8"x 1/16")
CrKα Radiation, V-filter, 2 mm Beam Slit, 35Kv 14mA
Strain Gage Reading = 300 micro-inches/inch

	$\Psi = 0^\circ$			$\Psi = 45^\circ$		
2θ	$2\theta_1$	$2\theta_2$	$2\theta_3$	$2\theta_1$	$2\theta_2$	$2\theta_3$
	156.1	156.2	156.3	156.0	156.1	156.2
Time for 100,000 counts in sec.	54.00	51.51	64.08	36.06	30.54	32.40
Correction factor (LP x Abs.)	1.04270	1.04235	1.04201	1.32460	1.32263	1.32066
Corrected times	56.306	53.691	66.772	47.765	40.393	42.789
	$a = 2.615$ $c = 0.1$			$a = 7.372$ $c = 0.1$		
	$b = 13.081$			$b = 2.396$		
$2\theta_{vertex}$	$(2\theta)_v = 2\theta_1 + c(\frac{3a + b}{2a + 2b})$			$(2\theta)_v = 2\theta_1 + c(\frac{3a + b}{2a + 2b})$		
	$= 156.1 + 0.067$			$= 156.0 + 0.125$		
	$= 156.167^\circ$			$= 156.125^\circ$		

Residual stress

$R.S. = K(2\theta_\perp - 2\theta_\Psi) = (86{,}300)\cdot(0.042) = 3{,}625$ psi

\+ Correction 3,000 psi

6,625 psi

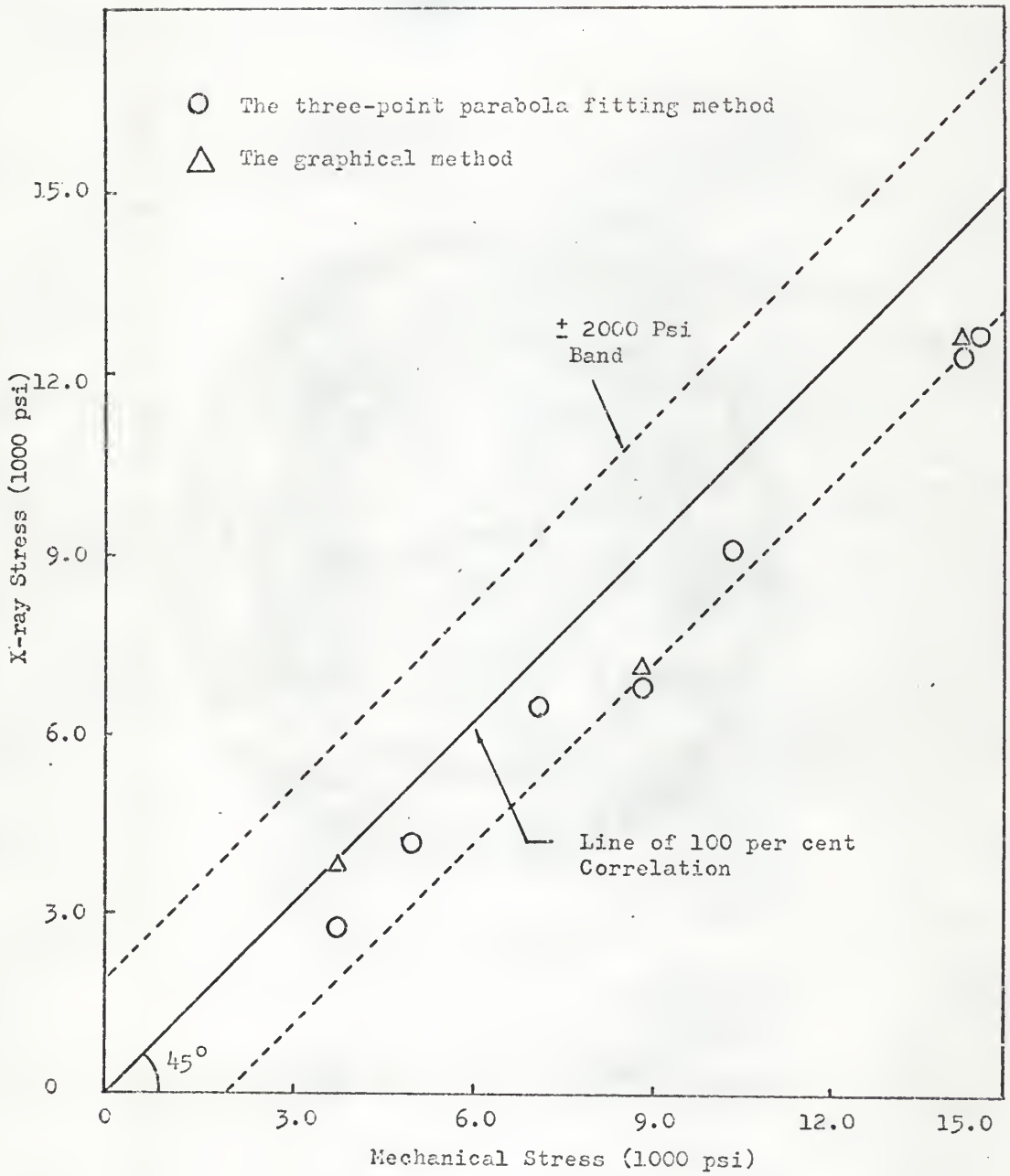

Fig. 7. Correlation data — X-ray stress versus mechanical stress.

steel, difficulties are commonly encountered if the diffraction lines are broad and diffuse. Since the X-ray method as applied to ordinary polycrystalline metals is essentially of the powder type, for mild steel or annealed metals where the grain size is relatively large, an anistropic response of groups of grains to applied stress may exist as indicated by Garrod (13). On this basis, variations between X-ray and bulk values for E and ν can be expected for annealed mild steel. For instance, it has been demonstrated that the X-ray stress factor is about 20 - 40 per cent higher than engineering values in hardened steels (8). For the better accuracy, it is desirable to evaluate the stress factor K experimentally. Calculation of the stress factor K using different elastic constants E and ν is given in Table 2. The stress factor K'= Kc was found to be 98,900 psi per 1° 2θ in this experiment using a least square fit of the data shown in Fig. 8. Referring to Table 2 this value of K is not unreasonable. The standard deviation was calculated to be 612 psi.

The absolute position of diffraction lines cannot be determined with certainty. However, in the X-ray stress measurement, it is only desired to determine the angular 2θ shift in the lines upon angular ψ rotation of the specimen with respect to the primary beam. If relative angular positions can be assigned to the diffraction peak, those positions suffice for the determination of stress. The need for resolving the $K\alpha_1\alpha_2$ doublet for a peak is of importance according to Finch (14). The practical doublets were shown in terms of the synthesized curves. This indicated the lack of coincidence between the $K\alpha_1$ peak and the apparent peak of the doublet. Because the intensity with high precision are usually taken at three points (e.g., angle interval 0.1° in the

Table 2

Calculation Of Stress Factor For
Specimen Angle $\psi = 45^{\circ}$

$$K = \frac{\cot \theta}{2} \cdot \frac{E}{1 + \nu} \cdot \frac{1}{\sin^2 \psi} \cdot \frac{\pi}{180}$$

Specimen Material	X-ray Target	Diffraction Peak 2θ (degree)	Lattice Planes	Poisson's Ratio ν	Young's Modulus $E \times 10^6$ psi	$\frac{E}{1 + \nu}$	Stress Factor K psi/1°2θ	Ref.
Steel	Cr	156.0	(211)	0.29	30	23.3	86,300	SAE TR-182
Iron	Cr	156.0	(211)	0.304[a]	36.36[b]	27.9	103,400	Donachie and Norton(17)
Mild Steel (1010)	Cr	156.0	(211)	—	—	26.7	98,900	Current work reported

[a] Averaged value. The range of value for given plane is 0.223 to 0.408.

[b] Averaged value. The range of value for given plane is 30.68 to 40.14.

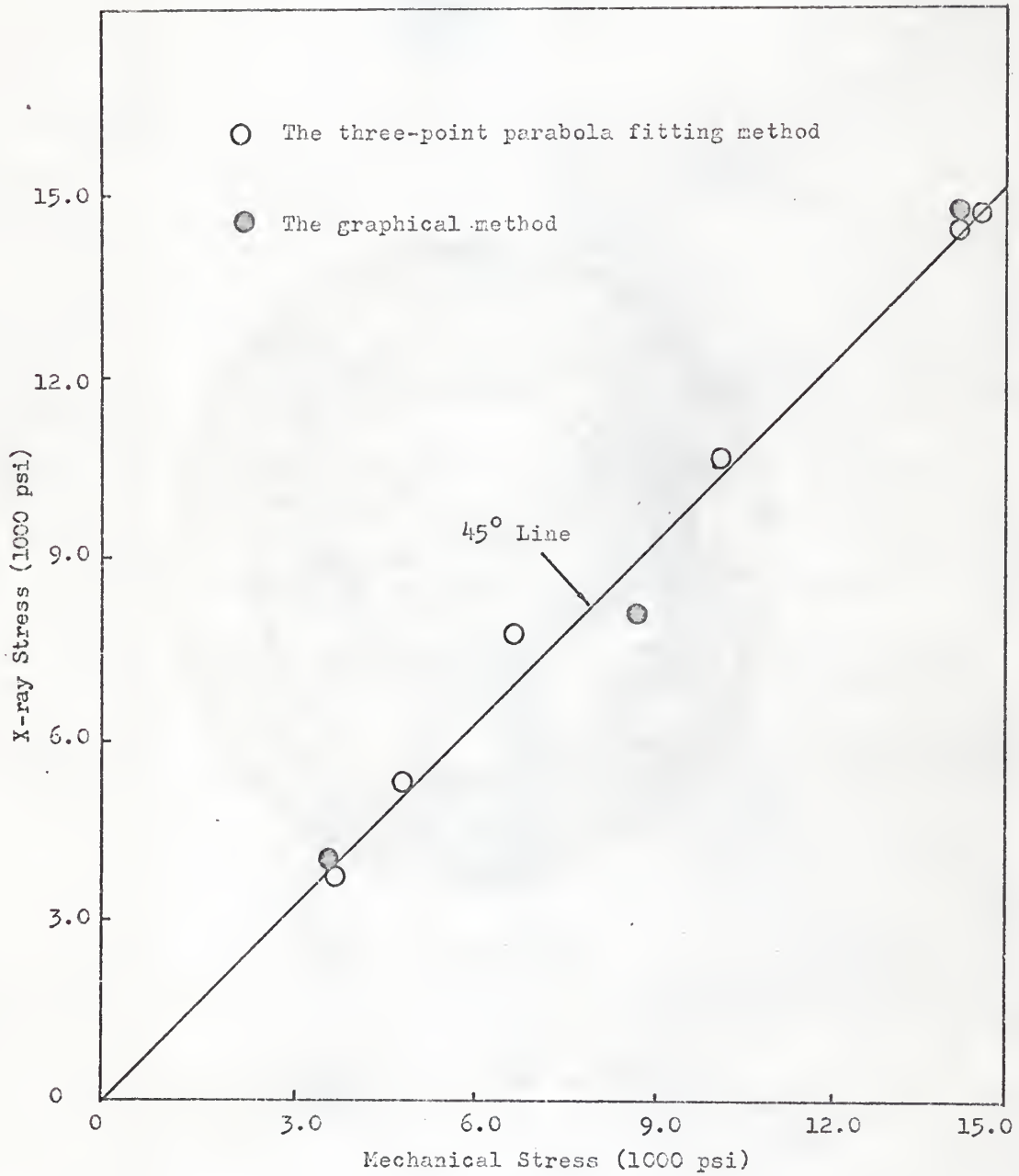

Fig. 8. The least square fit of the experimental data.

present work) straddling the peak and at least 80 per cent up from background, this choice of points can minimize the effect of poor resolution of the $K\alpha_1 - \alpha_2$ doublet.

The measured line intensities perhaps also ought to be corrected for background radiation. Since no simple method for properly correcting for background is now available, it has been customarily assumed that the background is composed of two components, one of constant intensity and another the intensity of which follows essentially the same 2θ relation as the diffracted beam (4). Under these conditions, no attempts had been made to correct for background in the present work. It has been stated that the correction factor (but not the anisotropy problem) may be ignored for mild steel where the $\alpha_1\alpha_2$ doublet is resolved and the angular width of the diffraction peaks is very small (8). This requirement was found to be met reasonably well by the sample used in this work. The peak locations were directly determined on the chart, with slow speed (e.g., $1/16^\circ$ per cm), by the graphical method and compared with those obtained from the three-point parabola fitting technique. The computed stresses are also given in Fig. 7. It was found that the graphical method correlated very well with the three-point parabola fitting technique. This indicates that no further corrections may be required to line measurement in the case of annealed mild steel.

From repeated measurements of the sample, it was found that stresses as determined by X-ray diffraction were about 1000 psi to 3000 psi too low. Also, with zero stress applied to the sample the X-ray measurements indicated that the sample was under compression as noted by a smaller 2θ angle for $\psi = 45^\circ$ than that for $\psi = 0^\circ$. The same type

of line shift was noted when the annealed steel filing sample was used. This 2θ angle difference was of the order of 0.01° and was assumed to be a result of diffractometer misalignment, however, this misalignment was too small to allow correction by further alignment procedures. Hence, a constant correction of 3000 psi was added to all measurements so as to place them more nearly on an absolute basis. This was necessary to bring the X-ray data into the coincidence with stresses computed from the strain gage readings.

For reliable X-ray stress measurement, the specimen surface must be clean and smooth. Any mechanical procedures for cleaning and smoothing, for instance abrading, grinding and metallographic polishing, etc., can disturb stresses at the surface and unfit for the successful measurement unless the disturbed layer is removed. It has been suggested that electropolishing is the most satisfactory method for smoothing or taking off stock (4). Mechanical procedures may also be used if the disturbed layer is thereafter removed by electropolishing, and acid etching is permissible to remove scale.

The coefficient of thermal expansion of iron is approximately $11 \times 10^{-6}/^{\circ}C$. It is apparent that large changes of temperature of the specimen must be avoided when small changes of Bragg angle are to be detected in the study of residual stress. In this case, the temperature of the fixture was constantly monitored at room temperature. Hence, any thermal expansion error was negligible.

Considerable information has been published on the application of X-ray in stress analysis. They include residual stresses in castings, forgings, welds, and heat-treated steel objects such as ball bearings and bearing races, machined and shot-peened surfaces. With

the help of X-ray method, it was found that the formation of residual subsurface stresses so called marstressing in a case-hardened mild steel (15). Many studies are being made with the plastically deformed materials. It has been demonstrated that when a bar is stretched plastically in tension and then unloaded, the observed shift in diffraction peaks indicated the presence of residual macroscopic compressive stresses at or near the surface. Mechanical methods indicated that there was no residual macrostress after unloading (i.e., removal of a layer from one surface did not produce curvature in the remainder of the bar)(5). Cullity (16) explained that this was due to a special distribution of microstress that was present.

In conclusion, the following may be summarized concerning the X-ray measurement of residual stresses on mild steel sheet, using the conventional formulas in computations.

(a) The X-ray residual stress measurement appeared readily reproducible with 2000 psi on mild steel sheet when a published stress factor (K = 86,300 psi per 1° 2θ) was used. Experimental stress factor K' was found to be 98,900 psi per 1° 2θ in the present work. The least square fit of the data yielded a standard deviation of 612 psi. Good correlation of X-ray and mechanically measured values (strain gage readings) was obtained. This indicates that elastic stresses can be directly related to the 2θ shift (or lattice strain) provided the constants of proportionality are known.

(b) Both the X-ray counter diffractometer and film camera can be used in the stress measurement of materials which yield sharp diffraction lines with excellent ratios of peak to background intensities. However, in materials providing broad or diffuse diffraction lines,

film techniques are unsatisfactory because proper corrections required for certain θ-dependent factors are difficult to apply to film blackening measurements.

(c) In the three-point parabola fitting technique, the parabolic approximation was valid when the parabola was fitted to the $K\alpha_1$ component of the $\alpha_1\alpha_2$ doublet. As a result, this technique has proved to be useful for rapidly determining the peak position whether the diffraction lines are sharp or diffuse.

(d) Advantages of the X-ray method include being able to measure stresses in thin layers, 2 or 3 ten thousandths of an inch thick. Also surface stresses can be measured nondestructively in contrast to the necessary dissection in the case of the mechanical methods. The X-ray method may also be used to make spot checks on a surface for uniformity or lack of stress.

(e) Limitations of the X-ray method arise chiefly from that imposed by the equipment and the size and shape of the piece rather than by the basic principles of the method. However, a disadvantage of the method is that both microstresses on the scale of grain size and macrostresses produced by external loads are measured; hence, it is impossible to separate stresses produced by processing from those produced by external loading (i.e., the method would not permit the evaluation of either stress individually, but merely their sum).

APPENDIX I

The Theoretical Developments of Stress Measurement By X-ray Diffraction Methods (4)

The basic principles involved are based on measuring strain which is then converted to the stress by equations developed in the classical theory of elasticity. The X-ray method as described herein will detect elastic strains only, as the method is fundamentally a measure of interatomic spacings, which are altered by elastic stresses. The classical theory of elasticity assumes the material whose state of stress is being measured is elastic, homogeneous and isotropic. Polycrystalline metals to a good approximation satisfy these requirements. The strain ε is defined as the unit change is length, that is:

$$\varepsilon = \frac{\Delta \ell}{\ell} \qquad \text{I-1.}$$

If the strain was produced by stress σ, acting in a single direction, Hooke's law requires that:

$$\varepsilon = \frac{\sigma}{E} \qquad \text{I-2.}$$

where E = Young's modulus. If a tensile stress σ_z is applied along the z direction, the metal will elongate along the z direction:

$$\varepsilon_z = \frac{\sigma_z}{E} \qquad \text{I-3.}$$

and contract equally along the x and y directions, and will be related to ε_z through Poisson's ratio as follows:

$$-\varepsilon_x = -\varepsilon_y = \nu \varepsilon_z = \frac{\nu \sigma_z}{E} \qquad \text{I-4.}$$

By principle of superposition we obtain:

$$\varepsilon_x = \frac{1}{E}\left[\sigma_x - \nu(\sigma_y + \sigma_z)\right]$$

$$\varepsilon_y = \frac{1}{E}\left[\sigma_y - \nu(\sigma_z + \sigma_x)\right]$$

$$\varepsilon_z = \frac{1}{E}\left[\sigma_z - \nu(\sigma_x + \sigma_y)\right] \qquad \text{I-5.}$$

The above equations relate the strain with an arbitrary set of axes, but may not represent the maximum stresses within the body, which are called principal stresses. The principal stresses σ_1, σ_2, and σ_3, however, can be made to correspond with the principal strains ε_1, ε_2, and ε_3, respectively, by arbitrarily selecting the coordinate axis in such a manner in the element of volume that the shear stresses on all the faces are zero, thus Eqs. I-5 can be rewritten to represent the principal strains and principal stress:

$$\begin{aligned}
\varepsilon_1 &= \frac{1}{E}\left[\sigma_1 - \nu(\sigma_2 + \sigma_3)\right] \\
\varepsilon_2 &= \frac{1}{E}\left[\sigma_2 - \nu(\sigma_3 + \sigma_1)\right] \qquad \text{I-6.} \\
\varepsilon_3 &= \frac{1}{E}\left[\sigma_3 - \nu(\sigma_1 + \sigma_2)\right]
\end{aligned}$$

If it is necessary only to determine the sum of the principal stresses in a surface by X-ray diffraction methods, a single photograph will suffice. The basis for computation will be Eqs. I-6. For example, assume the principal stresses $\sigma_1 + \sigma_2$ are in the surface plane, thus stress σ_3 which is normal to the free surface is zero, then:

$$\begin{aligned}
\varepsilon_3 &= \frac{1}{E}\left[0 - \nu(\sigma_1 + \sigma_2)\right] \qquad \text{I-7.} \\
\varepsilon_3 &= -(\sigma_1 + \sigma_2)\frac{\nu}{E}
\end{aligned}$$

To determine ε_3 it is merely necessary to measure the change in interplanar spacing of planes parallel to the surface by taking back-reflection diffraction patterns in the stressed (d_s) and unstressed condition (d_u):

$$\varepsilon_3 = \frac{\Delta \ell}{L} = \frac{d_s - d_u}{d_u}$$

$$(\sigma_1 + \sigma_2) = -\frac{E}{\nu}\left(\frac{d_s - d_u}{d_u}\right) \qquad \text{I-8.}$$

The above relationship relates the sum of the principal stresses, and is dependent upon the ability to measure the interplanar spacing both stressed and unstressed conditions. The sum of the principal stresses is usually of little value to the engineer; furthermore, it may be impossible to obtain the same material in the unstressed state (for example, hardened steels).

A more useful quantity is the surface stress in a desired direction, which can be determined from two exposures of the surface. One measurement of the interplanar spacing is made with the X-ray beam normal to the surface of the specimen whose stress is desired ($d_\perp$), and a second determination is made with the X-ray beam inclined at a known angle to the surface and lying in the vertical plane fixed by the surface direction of interest (d_ψ).

The interplanar spacings, $d_\perp$ and d_ψ, are related to the desired stress in the following manner:

Consider that the stress σ_φ is desired at point O in the φ direction of the metal plate of Fig. 9. It can be obtained from photographs taken along the z direction (perpendicular to the plate), and the ψ direction. The principal stresses σ_1, σ_2, and σ_3 are taken parallel to x, y, and z, respectively, and α_1, α_2, and α_3 are the components of direction cosines of the ψ direction relative to these axes. In terms of experimental angles ψ and φ, the components of direction cosines may be written:

$$\alpha_1 = \sin\psi\cos\varphi$$

$$\alpha_2 = \sin\psi\sin\varphi$$

$$\alpha_3 = \cos\psi = \sqrt{1 - \sin^2\psi} \qquad \text{I-9.}$$

The normal strain ε_n, in any chosen direction, is related to the principal strains ε_1, ε_2, and ε_3 by the components of direction cosines α_1, α_2, and α_3, respectively:

$$\varepsilon_n = \alpha_1^2\varepsilon_1 + \alpha_2^2\varepsilon_2 + \alpha_3^2\varepsilon_3 \qquad \text{I-10.}$$

and the stress:

$$\sigma_n = \alpha_1^2\sigma_1 + \alpha_2^2\sigma_2 + \alpha_3^2\sigma_3 \qquad \text{I-11.}$$

For the stress in the ψ direction, from Eqs. I-9 and I-11:

$$\sigma_\psi = \sigma_1(\sin\psi\cos\varphi)^2 + \sigma_2(\sin\psi\sin\varphi)^2 + \sigma_3\cos^2\psi \qquad \text{I-12.}$$

For σ_φ, when $\psi = 90^\circ$:

$$\sigma_\varphi = \sigma_1\cos^2\varphi + \sigma_2\sin^2\varphi \qquad \text{I-13.}$$

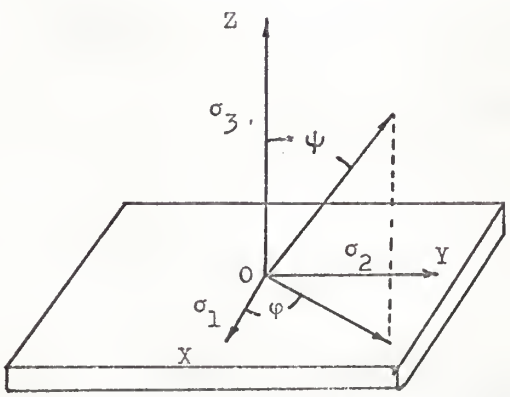

Fig. 9. Relation of chosen direction of stress to direction of principal stresses.

When Eq. I-9 is substitued into I-10, the strain is expressed in the ψ direction as:

$$\varepsilon_\psi = \varepsilon_1(\sin\psi\cos\varphi)^2 + \varepsilon_2(\sin\psi\sin\varphi)^2 + \varepsilon_3\cos^2\psi \qquad \text{I-14.}$$

Since the stress normal to a free surface is zero, $\sigma_3 = 0$, and the values of strain in terms of stress as expressed in Eq. I-5, then Eq. I-14 may be written as:

$$\varepsilon_\psi = \frac{1}{E}\left[(\sigma_1 - \nu\sigma_2)\cos^2\varphi\sin^2\psi + (\sigma_2 - \nu\sigma_1)\sin^2\varphi\sin^2\psi\right] + \varepsilon_3\cos^2\psi \qquad \text{I-15.}$$

which simplifies to:

$$\varepsilon_\psi - \varepsilon_3 = \frac{1+\nu}{E}(\sigma_1\cos^2\varphi + \sigma_2\sin^2\varphi)\sin^2\psi \qquad \text{I-16.}$$

Substituting Eq. I-13 into I-16 gives:

$$\sigma_\varphi = (\varepsilon_\psi - \varepsilon_3)\cdot\frac{E}{1+\nu}\cdot\frac{1}{\sin^2\psi} \qquad \text{I-17.}$$

The strain ε_ψ is equivalent to the difference in the interplanar spacing of the atomic planes in the stressed and unstressed conditions which lie perpendicular to ψ, thus:

$$\varepsilon_\psi = \frac{d_\psi - d_u}{d_u} \qquad \text{I-18.}$$

The strain ε_3 is equivalent to the difference in the interplanar spacing of the atomic planes in the stressed and unstressed conditions, which lie perpendicular to the z direction, thus:

$$\varepsilon_3 = \frac{d_z - d_u}{d_u} \qquad \text{I-19.}$$

Then:

$$\varepsilon_\psi - \varepsilon_3 = \frac{d_\psi - d_u}{d_u} - \frac{d_z - d_u}{d_u} = \frac{d_\psi - d_z}{d_u} \qquad \text{I-20.}$$

Since the interplanar spacing in the unstressed condition, d_u, is not determinable in most cases, to a close approximation this may be written as:

$$\varepsilon_\psi - \varepsilon_z = \frac{d_\psi - d_z}{d_z} \qquad \text{I-21.}$$

Substituting Eq. I-21 into I-17, the convenient equation for obtaining the stress from changes in interplanar spacing is obtained:

$$\sigma_\varphi = \frac{d_\psi - d_z}{d_z} \cdot \frac{E}{(1 + \nu)} \cdot \frac{1}{\sin^2\psi} \qquad \text{I-22.}$$

Instead of d_z, some textbooks use the notation $d_\perp$, since the determination of d_z (or $d_\perp$) involves planes which are almost parallel to the specimen surface, and during exposure the specimen is perpendicular to the primary X-ray beam in film work, or almost perpendicular in the case of the direct reading X-ray spectrometer.

The bulk of stress determinations by X-ray techniques is being conducted with X-ray spectrometer units, wherein the position of the diffracted beam is measured in terms of the angular position, 2θ, therefore, it is convenient to express the stress Eq. I-22 in terms of 2θ rather than the interplanar spacings.

Differentiating Bragg's law we obtain:

$$\frac{\Delta d}{d} = -\cot\theta \cdot \Delta\theta \qquad \text{I-23.}$$

which is equivalent to:

$$\frac{\Delta d}{d} = -\cot\theta \, \frac{\Delta 2\theta}{2} \qquad \text{I-24.}$$

Combining Eq. I-24 with Eq. I-22:

$$\sigma_\varphi = (2\theta_z - 2\theta_\psi) \frac{\cot\theta}{2} \cdot \frac{E}{(1 + \nu)} \cdot \frac{1}{\sin^2\psi} \qquad \text{I-25.}$$

or:

$$\sigma_\varphi = (2\theta_\perp - 2\theta_\psi) \frac{\cot\theta}{2} \cdot \frac{E}{(1 + \nu)} \cdot \frac{1}{\sin^2\psi}$$

For stress measurements on a given material, for example, hardened steel, the terms not involving the θ angle are constant and, therefore, Eq. I-25 can be expressed as:

$$\sigma_\varphi = K_1 \cdot \cot \theta \, (2\theta_\perp - 2\theta_\psi) \qquad \text{I-26.}$$

(θ expressed in radians.)

In practice, the cot θ term is also included into the constant, thus the final working equation used is:

$$\sigma_\varphi = K(2\theta_\perp - 2\theta_\psi) \qquad \text{I-27.}$$

where K = the stress factor.

APPENDIX II

Fitting Parabola To Three Points (12)

Having corrected the diffraction data for θ-dependent intensity factors, the peak position may be defined as the vertex of a vertical axis parabola fitted to the most intense portion of the diffraction peak. The calculation of the vertex of the parabola is greatly simplified if the parabola is fitted to three data points spaced at equal intervals on the x-axis.

The general equation of a parabola is:

$$(x - h)^2 = \alpha(y - k)$$

where α = constant and h, k are the coordinates of the vertex.

The three experimental points (x_1, y_1), $(x_1 + c, y_2)$, and $(x_1 + 2c, y_3)$ which lie on the parabola (Fig.10) determine three simultaneous equations:

$$(x_1 - h)^2 = \alpha(y_1 - k) \qquad \text{II-1.}$$

$$(x_1 + c - h)^2 = \alpha(y_2 - k) \qquad \text{II-2.}$$

$$(x_1 + 2c - h)^2 = \alpha(y_3 - k) \qquad \text{II-3.}$$

Solving Eqs. II-1 and II-2:

$$(x_1 + c - h)^2 - (x_1 - h)^2 = \alpha(y_2 - k) - \alpha(y_1 - k)$$

$$c^2 + 2x_1c - 2ch = \alpha(y_2 - y_1) = \alpha a \qquad \text{II-4.}$$

where: $a = y_2 - y_1$

Solving Eqs. II-2 and II-3:

$$(x_1 + c - h)^2 - (x_1 + 2c - h)^2 = \alpha(y_2 - k) - \alpha(y_3 - k)$$

$$-3c^2 - 2x_1c + 2ch = \alpha(y_2 - y_3) = \alpha b \qquad \text{II-5.}$$

where: $b = y_2 - y_3$

Solving Eqs. II-4 and II-5 for α and equating:

$$h = x_1 + \frac{c}{2}\left(\frac{3a + b}{a + b}\right)$$

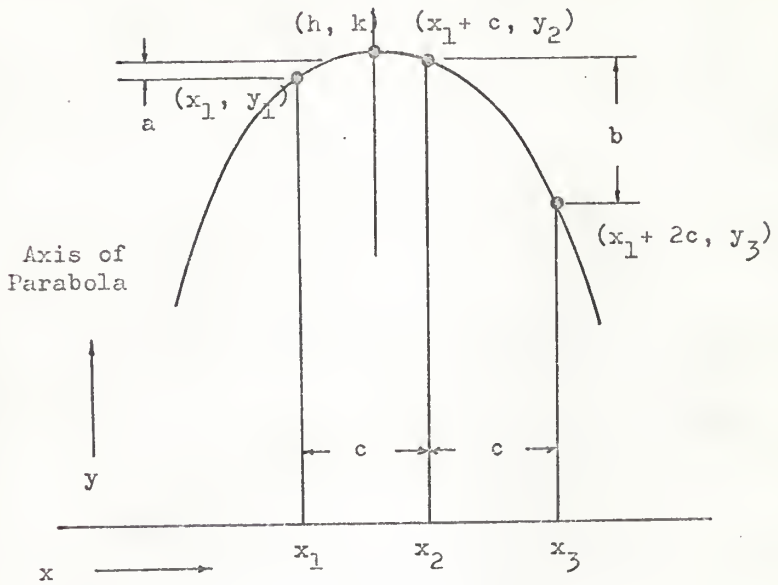

Fig. 10. Parabola fitted to three points.

$$\frac{c^2 + 2x_1c - 2ch}{a} = \frac{-3c^2 - 2x_1c + 2ch}{b}$$

$$-2x_1c(a + b) + 2ch(a + b) = 3ac^2 + bc^2$$

$$h = x_1 + \frac{c}{2}\left(\frac{3a + b}{a + b}\right)$$

where: h = Position on abscissa of vertex of parabola

x_1 = Position of first data point

c = Interval in x between data points

a, b = Differences in vertical coordinate (y) between middle data points and data points on either side of it.

This parabola-fitting technique works equally well if the y

coordinate is either intensity or time.

APPENDIX III

Calculation Of Absorption Factor (12)

The relative integrated intensities of X-ray beams diffracted by a specimen in a diffractometer can be calculated from basic general principles. The use of a flat plate specimen making equal angles with the incident and diffraction beams ($\psi = 0^\circ$) makes the absorption factor independent of the angle θ. For angles other than 0°, however, there will be a θ-dependent variation in the diffracted intensity due to absorption. Figure 11 shows a beam of intensity I_o of 1 sq. cm in cross-section incident on a metal surface at an angle α.

Consider the energy diffracted from this beam by a layer of length ℓ and thickness $d\underline{x}$, located at a depth $\underline{x}$ below the surface. Since the incident beam undergoes absorption by the metal over the path length AB, the energy incident on the layer is $I_o \exp\left[-\mu(AB)\right]$ where μ is the linear absorption coefficient. Letting $\underline{a}$ be the diffraction efficiency per unit volume, the energy diffracted by the layer of volume $\ell\, d\underline{x}$ is then $\underline{a} I_o \exp\left[-\mu(AB)\right] \ell\, d\underline{x}$. This diffracted beam is decreased by absorption through the path length BC. Thus the diffracted energy outside the specimen due to the layer is given by:

$$dI = \underline{a}\,\ell\, I_o \exp\left[-\mu(AB + BC)\right] d\underline{x} \qquad \text{III-1.}$$

But:

$$\ell = \frac{1}{\sin\alpha}\,, \quad AB = \frac{\underline{x}}{\sin\alpha}\,, \text{ and } BC = \frac{\underline{x}}{\sin\beta} \qquad \text{III-2.}$$

Therefore

$$dI_D = \frac{I_o \underline{a}}{\sin\alpha} \exp\left[-\mu\underline{x}\left(\frac{1}{\sin\alpha} + \frac{1}{\sin\beta}\right)\right] d\underline{x} \qquad \text{III-3.}$$

Since the angle ψ is most conveniently measured, the following substitutions are made: $\alpha = \theta + \psi$; $\beta = \theta - \psi$ III-4.

and thus:

$$dI_D = \frac{I_o \underline{a}}{\sin(\theta + \psi)} \exp\left[-\mu \underline{x}\left(\frac{1}{\sin(\theta + \psi)} + \frac{1}{\sin(\theta - \psi)}\right)\right] d\underline{x}$$

III-5.

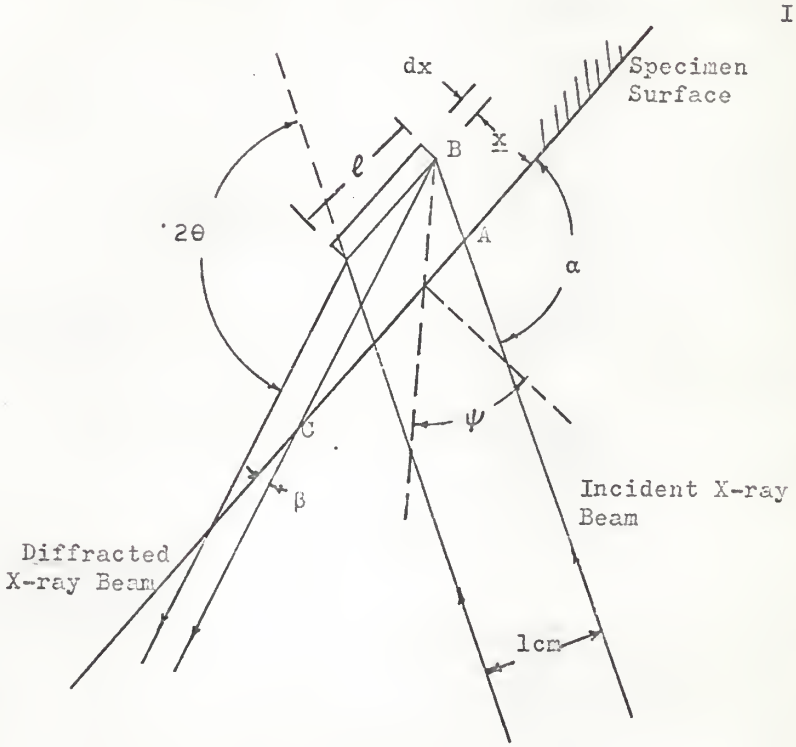

Fig. 11. Schematic representation of path of X-rays within sample.

The total diffracted energy is obtained by integrating over an infinitely thick specimen:

$$I_D = \int_{\underline{x}=o}^{\underline{x}=\infty} dI_D$$

$$= \int_o^\infty \frac{I_o \underline{a}}{\sin(\theta + \psi)} \exp\left[-\mu \underline{x}\left(\frac{\sin(\theta - \psi) + \sin(\theta + \psi)}{\sin(\theta + \psi) \cdot \sin(\theta - \psi)}\right)\right] d\underline{x}$$

$$= \frac{I_o \underline{a}}{\mu} \frac{1}{\sin(\theta + \psi)} \cdot \frac{\sin(\theta + \psi) \cdot \sin(\theta - \psi)}{\sin(\theta - \psi) + \sin(\theta + \psi)}$$

$$I_D = \frac{I_o a}{\mu} \quad \frac{\sin\theta\cos\psi - \cos\theta\sin\psi}{2\sin\theta\cos\psi}$$

Therefore:

$$I_D = \frac{I_o a}{\mu}(1 - \tan\psi\cot\theta) \qquad \text{III-6.}$$

and thus the θ-dependent absorption factor is: $1 - \tan\psi\cot\theta$.

APPENDIX IV

Correction Factors (4)

2θ	θ	1/(4.LP)	1/(4.LP.(45))
154.0	77.00	1.05032	1.36559
154.1	77.05	1.04994	1.36347
154.2	77.10	1.04957	1.36136
154.3	77.15	1.04919	1.35926
154.4	77.20	1.04882	1.35716
154.5	77.25	1.04845	1.35507
154.6	77.30	1.04808	1.35299
154.7	77.35	1.04772	1.35092
154.8	77.40	1.04735	1.34885
154.9	77.45	1.04698	1.34679
155.0	77.50	1.04662	1.34474
155.1	77.55	1.04626	1.34270
155.2	77.60	1.04590	1.34066
155.3	77.65	1.04554	1.33863
155.4	77.70	1.04518	1.33660
155.5	77.75	1.04482	1.33459
155.6	77.80	1.04446	1.33259
155.7	77.85	1.04411	1.33057
155.8	77.90	1.04375	1.32858
155.9	77.95	1.04340	1.32659
156.0	78.00	1.04305	1.32460
156.1	78.05	1.04270	1.32263
156.2	78.10	1.04235	1.32066
156.3	78.15	1.04201	1.31870
156.4	78.20	1.04166	1.31674
156.5	78.25	1.04132	1.31479
156.6	78.30	1.04097	1.31285
156.7	78.35	1.04063	1.31091
156.8	78.40	1.04029	1.30899
156.9	78.45	1.03995	1.30706
157.0	78.50	1.03961	1.30515
157.1	78.55	1.03927	1.30324
157.2	78.60	1.03894	1.30133
157.3	78.65	1.03861	1.29944
157.4	78.70	1.03827	1.29755
157.5	78.75	1.03794	1.29567
157.6	78.80	1.03761	1.29379
157.7	78.85	1.03728	1.29192
157.8	78.90	1.03696	1.29005
157.9	78.95	1.03663	1.28820
158.0	79.00	1.03630	1.28634

"LP" refers to the Lorentz-polarization factor of

$$\frac{1}{8} \cdot \frac{1 + \cos^2 2\theta}{\sin^2 \theta}$$

which is appropriate for measured intensities at specific points.
A cos θ factor (see Eq. 5) which appropriate only for integrated intensities has been omitted from the denominator.
"A" refers to the absorption factor of $(1 - \tan\psi \cot \theta)$. The number (45) in the column heading refers to the ψ angle for which the factor is applicable.
The measured intensities are to be multiplied by the factors tabulated.

APPENDIX V

Radiation Parafocus Settings In Millimeters For Psi Angles Of 45° And 60° At Various Two-theta Angles

Psi 45°

2θ	L (mm)	2θ	L (mm)
130.0	108.02	146.0	79.53
131.0	106.34	147.0	77.62
132.0	104.64	148.0	75.69
133.0	102.94	149.0	73.74
134.0	101.22	150.0	71.78
135.0	99.49	151.0	69.79
136.0	97.75	152.0	67.78
137.0	95.99	153.0	65.75
138.0	94.22	154.0	63.70
139.0	92.44	155.0	61.63
140.0	90.64	156.0	59.54
141.0	88.83	157.0	57.42
142.0	86.99	158.0	55.27
143.0	85.16	159.0	53.10
144.0	83.30	160.0	50.91
145.0	81.42		

Psi 60°

2θ	L (mm)	2θ	L (mm)
150.0	107.65	155.5	92.80
150.5	106.36	156.0	91.37
151.0	105.06	156.5	89.93
151.5	103.74	157.0	88.48
152.0	102.42	157.5	87.01
152.5	101.08	158.0	85.53
153.0	99.73	158.5	84.03
153.5	98.37	159.0	82.51
154.0	96.99	159.5	80.98
154.5	95.61	160.0	79.44
155.0	94.21		

$$L = R - R\,\frac{\cos(\psi + \varphi)}{\cos(\psi - \varphi)}, \quad \varphi = 90^{\circ} - \theta$$

where R = Source to sample distance, or radius of goniometer circle (=170 mm),

L = Distance that the counter must be moved toward the center of goniometer.

REFERENCES

1. Orowan, E. Symposium on Internal Stresses in Metals and Alloys, Inst. Metals, London, p. 4, 1948.

2. Denton, A. A. Determination of Residual Stresses, Metallurgical Reviews 101, 11, p. 1, 1966.

3. ASM Committee. Residual Stresses, Metals Handbook, Am. Soc. for Metals, Supplement, Cleaveland, p. 89, 1955.

4. Christenson, A. L. ed., Measurement of Stress by X-ray, SAE Inform Rept. TR-182, The Soc. Automotive Eng., New York, 1960.

5. Barret, C. S. and Massalski, T. E. Structure of Metals, 3rd ed., McGraw-Hill Book Co., Inc., New York, p. 466, 1966.

6. Newton, C. J. Residual Stresses and Their Relaxation on the Surfaces of Sections Cut from Plastically Deformed Steel Specimen, J. Research Nat. Bur. Stand., (C)67, p. 101, 1963.

7. Donachie, M. J., Jr. and Norton, J. T. Residual Stresses in Shot-peened Aluminum Bars, Proc. Soc. Exper. Stress Anal., XIX, No. 2, p. 222, 1966.

8. Beu, K. E. An Evaluation of Geiger Counter X-ray Techniques for Measuring Stresses in Hardened Steels, Am. Soc. for Testing Materials Proc., 57, p. 1282, 1957.

9. Klug, K. P. and Alexander, L. E. X-Ray Diffraction Procedures, John Wiley and Sons, Inc., New York, p. 101, 1954.

10. Christenson, A. L. and Rowland, E. S. X-ray Measurement of Residual Stress in Hardened High Carbon Steel, Trans. ASM, 45, p. 638, 1953.

11. Cullity, B. D. Elements of X-Ray Diffraction, Addison Wesley Pub. Co., Inc., p. 431, 1956.

12. Koistinen, D. P. and Marburger, R. E. A Simplified Procedure for Calculating Peak Position in X-ray Residual Stress Measurement on Hardened Steel, Trans. ASM, 51, p. 537, 1957.

13. Garrod, R. I. Residual Lattice Strains in Mild Steel, Nature, No. 4189, p. 241, 1950.

14. Finch, L. G. A Correction to Diameter Measurement of Diffuse X-ray Diffraction Rings, Nature, No. 4141, p. 402, 1949.

15. Search, March 1965, Research Laboratories, General Motors Corp.

16. Cullity, B. D. Residual Stress After Plastic Elongation and Magnetic Losses in Silicon Steel, Trans. Met. Soc. AIME, 227, p. 356, 1963.

17. Donachie, M. J., Jr. and Morton, J. T. X-ray Studies of Lattice Strains Under Elastic Loading, Trans. ASM, 55, p. 51, 1962.

ACKNOWLEDGMENTS

The author wishes to express his sincere appreciation to Dr. A. E. Hostetter for his guidance and encouragement. Without his assistance this work would not have been accomplished. Appreciations are also extended to Mr. K. N. Hearn, who guided the experimental work, Dr. F. J. McCormick, who aided in the preparation of strain gages on the specimen, and Drs. F. A. Tillman and R. D. Dragsdorf, who offered many valuable suggestions.

X-RAY MEASUREMENT OF RESIDUAL STRESSES

by

MYUNG CHUL KIM

B. S., Seoul National University, 1964

AN ABSTRACT OF A MASTER'S THESIS

submitted in partial fulfillment of the

requirements for the degree

MASTER OF SCIENCE

Department of Industrial Engineering

KANSAS STATE UNIVERSITY
Manhattan, Kansas

1968

X-ray residual stress measurement of mild steel sheet was discussed. The techniques are based on the two-exposure method and the use of counter diffractometer. A simple fixture was utilized to apply a mechanical strain to a specimen which was then measured both X-ray diffraction and electric resistance strain gages. The radiation employed was the $K\alpha_1$ of chromium, and all measurements were exclusively taken on the 211 diffraction line. It was found that the combined errors of both X-ray method and strain gages reading produced maximum deviation of just over 2000 psi when a published value of stress factor (e.g., K = 86,300 psi per $1^{\circ}2\theta$) was used. An experimental stress factor was found to be 98,900 psi per 1° 2θ in the present work using a least square fit of the data. The standard deviation was calculated to be 612 psi. Good correlation of X-ray and mechanically measured values was obtained.